35th Annual International Conference of the IEEE EMBS
Osaka, Japan, 3 - 7 July, 2013

Evaluation of a 3D Technique for Quantifying Neovascularization within Plaques Imaged by Contrast Enhanced Ultrasound

Assaf Hoogi, Grigoriy Zurakhov and Dan Adam, *Senior Member, IEEE*

Abstract - **Intra-plaque neovascularization and inflammation are considered as important indicators of plaque vulnerability, which when ruptured, may cause stroke or acute myocardial infarction.**

The purpose of this research was to validate and evaluate a semi-automatic method, which allows quantification of carotid plaque neovascularization using contrast-enhanced ultrasound cines, thus enabling assessment of plaque vulnerability. The method detects contrast clusters in the images, and tracks them, to generate over time a path that portrays the neovasculature. It classifies the paths as either artifacts or 'blood vessels' and reconstructs the 3D arterial tree.

Software-based phantom was developed to represent volumetric structures of the carotid lumen, the plaque, and 'objects' passing through the intra-plaque neovasculature. These 3D objects, which mimic microbubbles or clusters of microbubbles, were based on original 2D formations, imaged during clinical examinations using contrast-enhanced ultrasound. Within a plaque, several paths were constructed, representing flow inside blood vessels, and several isolated objects were added, representing artifacts. Different paths were generated, classified into 4 groups: separate paths, paths that merge at some point, paths that branch and intersecting paths.

The phantom was used to generate sets of cines, which were then processed by the method. The method identified artifacts and different paths, which were then compared to the 'true' ones. Sixty-four 'objects' in 16 movies were examined. All of them were detected. 79% of those objects were well tracked and classified to either artifacts or real blood vessels.

The results of this study show that the method accurately identifies artifacts and paths, which allows reconstruction of intra-plaque vascular tree and quantification of the plaque neovasculature, which is associated with plaque vulnerability.

Keywords: Neovascularization, 3D Quantitative analysis, Software-based phantom

I. INTRODUCTION

Cardiovascular events are considered as the leading cause of death in the developed countries. Many of these events are associated with plaque development and plaque vulnerability. In recent years, studies of the relationship between atherosclerosis and stroke or myocardial infarction have concentrated on the presence of neovascularization and inflammation in the atheromatous plaque as reliable markers of vulnerability of the plaque. Studies indicate that neovascularization is regularly seen in atherosclerotic plaques [1], when imaged by contrast enhanced ultrasound (CEUS). It was also shown that plaque rupture is well associated with the presence and degree of neovascularization within the plaque [2].

Therefore, the ability to detect and quantify the amount of neovascularization in the plaque by using a noninvasive method is of major clinical interest. Several papers present a semi-quantitative visual assessment of intra-plaque neovascularization using contrast-enhanced ultrasound images [3], generally by using a discrete grading system. In [4], a semi-quantitative grading system based on visual interpretation alone is used. Those grading levels include absence of neovascularization (grade 0) to high echogenicity (grade 3) caused by a high amount of contrast agent enhancement. Measurements of plaque echogenicity by gray level and entropy have also been reported as possible markers of risk of plaque rupture [5]. However, as far as we know, only [6-7] presents a semi-automatic algorithm to quantify the neovascularization inside the plaque, using an accumulative image of the neovascularization over several heart cycles. Moreover, it is difficult to locate other studies, except for [7], which describe an objective method for a semi-automatic quantitative analysis of neovascularization in the atheromatous plaque based on the 2D behavior of contrast bubbles over time. However, there are hardly any reports describing the 3D behavior of the contrast clusters over time, depicting the 3D structure of the neovascularization within the plaque, and evaluating these results.

II. MATERIAL AND METHODS

A. Contrast imaging

Ultrasound contrast agent Sonoview (Bracco, Geneva, Switzerland) was injected to obtain contrast 2D images. The contrast material contains encapsulated bubbles (few micron in size) that can flow through the small neovascularization within the plaque. 2nd harmonic imaging was used to optimize the contrast enhanced ultrasound (CEUS) imaging.

B. Software-based phantom

A software-based 3D model was constructed based on contrast enhanced 2D cine obtained during a clinical examination [7]. Fifty 2D frames were extracted. They included the carotid lumen and a plaque. Temporal linear interpolation between those frames was applied to create one

*Resrach supported by Technion-VRP and the Ultrasound Imaging Lab.

A. Hoogi, Grigoriy Zurakhov and D. Adam are with the Dept. of Biomedical Engineering, Technion – IIT, Haifa 32000, Israel (corresponding author phone: 972-4-829-4114; fax: 972-4-829-4599; e-mail: ahoogi@gmail.com).

thousand images. The interpolation was done to obtain a sufficient number of volume units. These images were divided into 20 volume units, 50 frames each (each of these fifty was considered as a specific z-layer within the same volume unit). Therefore, the size of each XYZ volume unit was [140, 140, 50] pixels. These volume units were stacked together, thus considered as 20 new 3D frames that composed the whole volume. In some of those fifty Z layers in each volume unit, intra-plaque objects, either artifacts or blood vessels, were located.

3D bubbles were constructed by using 2D images of the original bubbles that were extracted from the original cine. Bubbles of 2 sizes were created: 9x9 pixels and 6x6 pixels. Because a bubble should have a symmetrical 3D scattering, it was constructed by extracting a 2D image of the original bubble, placing it on both X and Y symmetry axes and manually filling the rest of the remaining pixels in the 3D matrix in a way that maintains a spherical spatial symmetry.

In Figure 1, one can see the images of an 2D original bubble placed on 2 planes symmetrically around the XY axes, and the sphere constructed manually filled to demonstrate the spherical scattering from a bubble.

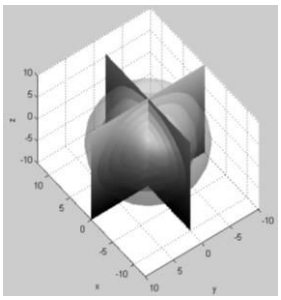

Figure 1: Reconstruction of a 3D bubble. 2D image of a bubble was projected on 2 planes on the X and Y symmetry axes. A surrounding sphere was manually constructed to demonstrate the spherical scattering from a bubble

Artifacts and bubbles were placed in determined coordinates within the first volume unit. Each bubble cluster was characterized by size, gray level distribution and spatial location. The values of these parameters were modified between sequential volume units. The size of each cluster could be slightly changed between these volume units by randomly subtracting [0 2] pixels from each axis. Its gray level distribution was changed by adding to each pixel a random value from the predetermined symmetric interval of [-5 5] gray levels. The step size of each cluster between one volume unit to another was randomly selected from the interval of [-2 2] pixels for each axis independently. The range of values was determined according to typical values that were measured during clinical examinations. Artifacts which are characterized by negligible movement were designed to move randomly within an interval [-1 1] pixels along each axis.

Several simulations were performed, describing different paths and objects: separate paths that represent intra-plaque blood vessels, paths that merge at some point, branching paths and paths that cross one path over the other.

The most significant advantage of a 3D model dataset is the possibility to demonstrate the ability of the technique for quantifying the neovascularization to distinguish between merging/branching paths and those paths that just cross each other. These two different cases sometimes cannot be separated when 3D movement is projected onto a 2D plane. When an intersection is viewed in a 2D plane, it may be an intersection, while the 3D data may reveal that the paths actually lie at different Z layers, which the 3D algorithm should identify. Figure 2a shows 2 blood vessels that contain 3 bubbles (green colored) that seem to intersect. However, by rotating the image one can see an additional bubble that was hidden in Figure 2a, that describes a path that does not intersect with the first one.

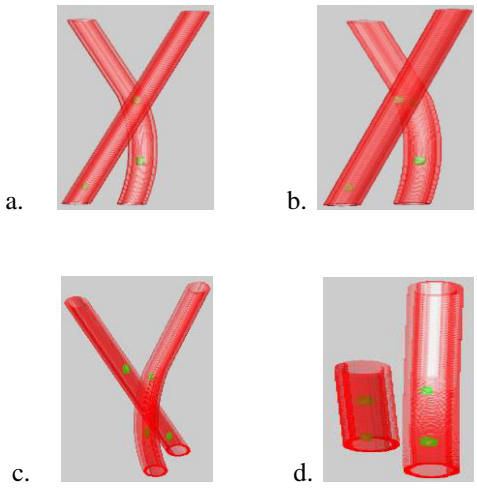

Figure 2: Illustration of several bubbles (green colored) within 2 intra-plaque blood vessels (red colored) at different angles. It demonstrates the advantage of 3D volumetric data over 2D data. (a) An inclusion between those 2 blood vessels. (b-d) Different angles show that in 3D space these are vessels that can be analyzed separately.

The last step of the construction of the model includes the addition of speckle noise (Mean 0, Variance 0.1).

C. Technique for Quantifying Neovascularization

Contrast spot detection. The technique for quantifying the neovascularization employs a 3D artificial template, for detection of contrast-like objects. The detected objects are combined to form the intra-plaque contrast accumulations. The spherical template is constructed resembling a typical pattern of real contrast spots, as well typical 'radius' and varying gray levels with spherical symmetry. Radii of 3, 5 and 7 (for each of the X, Y, Z axes) are considered. The detected spots are combined to obtain the final object detection.

Maximal intensity was determined at the center point of the sphere and decreased as a function of the distance from that point. The artificial template was compared to all

positions within the plaque volume using normalized cross correlation. A correlation coefficient matrix was calculated and correlation values above 0.8 were considered as object locations.

The location of the maximal correlation within the whole reconstructed volume was detected and a surrounding neighborhood of 5*5 pixels was deleted from that volume. This iterative process continued till the maximal correlation value was below 0.8.

Bubble tracking by Dynamic Programming. Tracking bubbles' accumulations enables arterial tree reconstruction of thse intra plaque vessels and a more accurate analysis. Dynamic Programming (DP) is an optimal approach for solving variational problems by finding locally optimal solutions consecutively. The task was to track the three-dimensional displacement of a bubble within the plaque over time. This corresponds to finding a connective path, as the function of time, through a four-dimensional (X,Y,Z,T) matrix, with minimal total cost, using multidimensional DP [8].

The process started at the first volume unit, at XYZ locations in which the objects were detected for the first time, and continued forwards till the last volume unit. The resulting optimal path was determined by the following parameters: cost (correlation values) and path smoothness (allowing step size and side step penalty)

1) Correlation values: Normalized Cross Correlation (NCC) was applied to track the objects within the vasculature of the carotid plaque, due to its insensitivity to local variations in the mean and standard deviation (SD) of the image gray level (which are very common in contrast accumulations). For each object, a template of 19*19*19 pixels around its center was placed. This template was correlated for all volume units with target image blocks, which were extracted from a search area of 51*51*51 pixels, centered at the location of the detected object in the first volume unit. The size of the search area should be large enough to accommodate the maximal displacement over the US cine, without leading to an unnecessary computational load [9]. NCC is optimal when it is close to its maximal value of 1.0. To use NCC properly in the multidimensional DP minimization task, a cost function $(1-NCC)^{1/3}$ was used (Eq. 1, expression 1a).

2) Step size: the connectivity of the graph should fit the maximum distance that a contrast accumulation could transpose between two sequential volume units. The maximal step size is 3 pixels in each direction (X,Y,Z), large enough to handle the possible motion of bubbles flow. Furthermore, temporal smoothness of the motion was controlled by expression 1b. [8,9]. Step size of an examined spot moving between 2 unit volumes is presented as $\Delta x, \Delta y, \Delta z$ and the cost function is depicted by f_x, f_y, f_z (eq.1)

$$F(x,y) = \underbrace{(1-NCC)^{1/3}}_{1a} \left\{ \underbrace{(1/f_x)^{\Delta x} + (1/f_y)^{\Delta y} + (1/f_z)^{\Delta z}}_{1b} \right\} \quad (1)$$

The optimal path was extracted by finding the minimal cumulative cost value in the last volume unit, and tracking backwards to the beginning, through minimal values over the cumulative cost matrix. The result was a globally optimal path [9]. Reconstructing the final path was possible only after arriving to the last volume unit, and using the accumulated cost, instead of determining the contrast location in each frame (as applied in forward tracking), which made the method less sensitivity to noise and correlation errors.

D. Algorithm validation

Comparisons to visual analysis and to paths that were generated by simulations (using the phantom described above) were performed to validate the algorithm . An external observer visually examined the objects that were detected within the whole first volume unit. False positive and false negative cases were examined. The tracking results that were obtained by the algorithm were compared to the paths that were generated directly by the software-based phantom.

III. RESULTS

Several interactions between objects were generated: paths of the accumulations that represent separate intra-plaque blood vessels, paths that merge at some point, branching paths and paths that cross one path over the other.

Sixty-four 'objects' in 16 movies were examined. In each plaque, 2 contrast accumulations represented bubbles which move over the time, while another 2 spots represented artifacts. All objects were well detected within the first unit volume and their XYZ location was accurately obtained.

Figure 3(a-b) presents two original images that were extracted from the first volume unit, as an example of the object detection process. In Fig. 3(c-d), two objects were detected within the plaque (marked by red and green crosses). There are also 2 artifacts in this plaque that were also detected (yellow circled). It is worth mentioning that the objects are presented in 2 different images due to their locations within various z layers of the volume unit.

a. 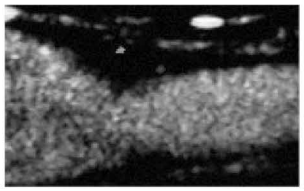 b. 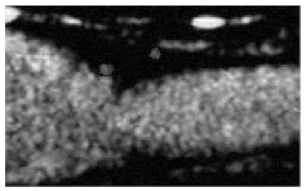

c. 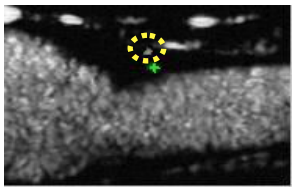 d. 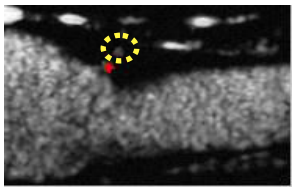

Figure 3: Object detection at two different Z layers of the first volume unit. (a-b) Original images that were extracted from the first volume unit. (c-d) The objects that represent bubble accumulations are red and green colored while the artifacts are marked by yellow circles.

79% of the objects were well tracked over the volume units. Figure 4 shows the paths that were generated for each object in Fig. 3, due to its movement in time. It shows a comparison between those paths that were generated by the software-based phantom and those detected by the algorithm. High tracking accuracy was determined when the mean distance between these paths was less than 3 pixels (~0.3mm).

a. 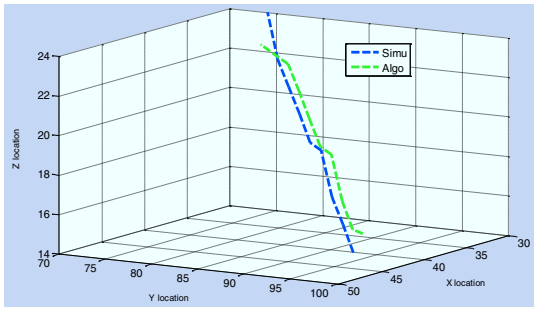

b. 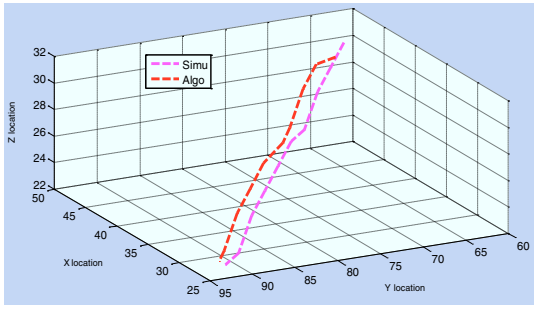

Figure 4: Comparison between the paths that were generated by the simulation and the tracking results obtained by the algorithm. (a) Tracking the object that was detected in Fig. 3c. (b) Tracking the object that was detected in Fig. 3d

Classification to artifacts and real blood vessels was performed based on a 4 mm threshold of XYZ displacement. All 79% well tracked objects were accurately classified.

IV. Discussion

A semi-automatic method for 3D quantification of the intra-plaque neovascularization, which requires minimal user interaction, has been here validated. The method is robust to noise and small disturbances. It was applied to 64 cases in 16 movies that were generated by the software-based phantom.

The method has several advantages for quantifying the neovascularization. First, it exploits the DP advantages: relative insensitivity to noise and small disturbances, efficient, and producing a time continuous motion [10]. We have performed validation of the detection process against our visual interpretation. The tracking validation was done by comparing the method's results to the paths that were generated by the simulation.

V. Conclusion

Tools have been developed for 3D quantification of neovascularization in carotid plaques, and have here been validated. They include a semiautomatic technique for detecting the 3D contrast spots in the plaque, tracking such spots over time by MDP and classifying them into artifacts and vessels. Preliminary evaluation shows promising results.

VI. References

[1] A.C. Barger, R.3rd Beeuwkes, L. L. Lainey, and K.J. Silverman, "Hypothesis: vasa vasorum and neovascularization of human coronary arteries: a possible role in the pathophysiology of atherosclerosis," *NEngl J Med*, vol. 310, 1984 , pp. 175–177.

[2] M. Fleiner, M. Kummer, and M. Mirlacher, "Arterial neovascularization and inflammation in vulnerable patients: early and late signs of symptomatic atherosclerosis, " *Circulation,* vol. 110, 2004, 2843–2850.

[3] S. Coli, M. Magnoni, G. Sangiorgi, M. M. Marroco-Trischitta, G. Melisurgo, A. Mauriello, L. Spagnoli, R. Chies, D. Cianflone and A. Maseri, "Contrast enhanced ultrasound imaging in intra plaque neovascularizationin carotid arteries: correlation with histology and plaque echogenicity, " *J Am Coll Cardiol,,* vol. 52, 2008, pp. 223–230.

[4] F. Shah, P. Balan, and M. Weinberg, "Contrast-enhanced ultrasound imaging of atherosclerotic carotid plaque neovascularization: a new surrogate marker of atherosclerosis?, "*VascMed,* vol. 12, 2007, pp. 291–297.

[5] T. G. Papaioannou, M. Vavuranakis, and A. Androulakis, "In-vivo imaging of carotid plaque neoangiogenesis with contrast enhanced harmonic ultrasound," *Int J Cardiol*, vol. 134, 2009, pp. e110–e112.

[6] A. Hoogi, D. Adam, A. Hoffman, H. Kerner, S. Reisner, and D. Gaitini, "Carotid plaque vulnerability: Quantification of neovascularization on Contrast-Enhanced Ultrasound With Histopathologic Correlation," *AJR*, vol. 196, 2011, pp. 431-436.

[7] A. Hoogi, Z. Akkus, S. C. van den Oord, G. L. Ten Kate, A. F. Schinkel, J. G. Bosch, N. de Jong, D. Adam and A. F. van der Steen, "Quantitative analysis of ultrasound contrast flow behavior in carotid plaque neovasculature," *Ultrasound Med Biol*, vol. 38(12) , 2012, pp. 2072-2083,2012.

[8] S. T. Nevo, M. Van Stralen, A. M. Vossepoel, J. H. C. Reiber, N. de Jong, A. F. W van der Steen, and J. G. Bosch, "Automated tracking of the mitral valve annulus motion in apical echocardiographic images using multidimensional dynamic programming," *Ultrasound in medicine & biology*, vol. 33(9), 2007, pp. 1389-1399.

[9] M. U¨zümcü, R. J. van der Geest, C. Swingen, J. H. C. Reiber, and B. P. F. Lelieveldt, "Time continuous tracking and segmentation of cardiovascular magnetic resonance images using multidimensional dynamic programming, " *InvestRadiol,,* vol. 41, 2006, pp. 52– 62.

[10] S. I. Rabben, A. H. Torp, A. Støylen, S. Slørdahl, K. Bjørnstad,B. O. Haugen, and B. Angelsen, "Semiautomatic contour detection in ultrasound m-mode images, " *Ultrasound Med Biol*, vol. 26, 2000, pp. 287– 296.